Electronic excitations around the substituted atom in $La_2Cu_{1-y}Ni_yO_4$ as seen via resonant inelastic x-ray scattering

K. Ishii,[1] K. Tsutsui,[1] K. Ikeuchi,[1] I. Jarrige,[1] J. Mizuki,[1] H. Hiraka,[2] K. Yamada,[2,3] T. Tohyama,[4] S. Maekawa,[5] Y. Endoh,[1,6] H. Ishii,[7] and Y. Q. Cai[7,8]

[1]*SPring-8, Japan Atomic Energy Agency, Hyogo 679-5148, Japan*
[2]*Institute for Materials Research, Tohoku University, Sendai 980-8577, Japan*
[3]*Advanced Institute for Materials Research (WPI), Tohoku University, Sendai 980-8577, Japan*
[4]*Yukawa Institute for Theoretical Physics, Kyoto University, Kyoto 606-8502, Japan*
[5]*Advanced Science Research Center, Japan Atomic Energy Agency, Tokai 319-1195, Japan*
[6]*International Institute for Advanced Studies, Kizu, Kyoto 619-0025, Japan*
[7]*National Synchrotron Radiation Research Center, Hsinchu Science Park, Hsinchu 30076, Taiwan*
[8]*National Synchrotron Light Source II, Brookhaven National Laboratory, Upton, New York 11973, USA*

(Received 21 December 2011; revised manuscript received 19 February 2012; published 14 March 2012)

We perform a resonant inelastic x-ray scattering (RIXS) study of Ni-substituted La_2CuO_4 and Cu-substituted La_2NiO_4. Resonantly enhanced charge-transfer excitations are successfully observed by tuning the incident photon energy to the K edge of the substituted element. These excitations display a very weak momentum dependence, evidencing their local character. We find a shift in the energy of the onset edge of these features compared with the nonsubstituted compounds La_2CuO_4 and La_2NiO_4. This shift is quantitatively reproduced by exact diagonalization calculations of the RIXS spectra. RIXS is shown to be a powerful tool to probe the electronic states of substituted elements and to understand their interaction with surrounding atoms.

DOI: 10.1103/PhysRevB.85.104509 PACS number(s): 74.25.Jb, 74.62.Dh, 74.72.−h, 78.70.Ck

I. INTRODUCTION

Chemical substitution for a specific element is often used in the study of high-T_c superconducting cuprates. The best-known purpose of the substitution is to control the carrier concentration in the CuO_2 plane, e.g., as in $La_{2-x}Sr_xCuO_4$ and $Nd_{2-x}Ce_xCuO_4$. One can also investigate the effect of disorder on the superconducting properties by partially substituting an isovalent cation with different ionic size for the one in the blocking layer.[1,2] On the other hand, the substitution for Cu can yield direct insight into the role of Cu atoms in superconductivity and has thus been the subject of intense scrutiny.[3] It was found that the substitution affects the superconductivity significantly and results in an abrupt reduction of the transition temperature.[4,5] The substitution by Ni and Zn is of particular interest since both Ni and Zn are considered to be divalent as Cu with a spin of, respectively, $S = 1$ and 0, so that the substitution seemingly changes only the spin magnetic moment of the Cu site. Nonetheless, it was later suggested that this picture is too simplistic;[6–12] namely, the changes of the local electronic states at the substituted site should also be taken into account in order to properly understand the substitution effect. In order to study these changes, local and/or element-selective experiments are indispensable.

One possible technique is scanning tunneling spectroscopy. Due to the atomic-scale resolution one can select the substituted atom and measure its local electronic states. Impurity states with an energy scale comparable to the superconducting gap have been argued.[13,14] Another appropriate experimental technique to investigate local electronic structure is core-level x-ray spectroscopy. By tuning the x-ray energy to the core-electron level of an element, one can obtain element-selective spectra. As such a technique, x-ray absorption near edge structure (XANES) allows one to gain information about the unoccupied states. With the availability of brilliant light sources, it has recently become possible to measure charge excitations near the Fermi energy in an element-selective way using resonant inelastic x-ray scattering (RIXS),[15,16] thereby opening a route to access both occupied and unoccupied states. This, plus the fact that the final state of RIXS does not suffer from core-hole effects in contrast to XANES, makes RIXS particularly well suited to the study of substituted elements.

In this study we report on the use of RIXS at the absorption edge of substituted elements and demonstrate the unique capability of the technique to measure local electronic excitations around these elements. We start here with simple samples, carrier-undoped $La_2Cu_{0.95}Ni_{0.05}O_4$ and its counterpart $La_2Cu_{0.05}Ni_{0.95}O_4$, measured, respectively, at the Ni and Cu K edges. By comparing the spectra with those of nonsubstituted La_2CuO_4 and La_2NiO_4, we find that the onset edge of the feature corresponding to charge-transfer (CT) excitation is shifted by ∼0.5 eV. This shift is quantitatively reproduced by exact diagonalization calculations based on a d-p model, and its origin is attributed to modifications of the unoccupied states of the substituted element. RIXS on substituted elements is shown to be a powerful tool not only for detecting the presence of these elements, but also for finely probing their electronic states affected by the interaction with surrounding atoms.

II. EXPERIMENTAL DETAILS

RIXS experiments were performed at the Taiwan inelastic x-ray scattering beamline (BL12XU) at SPring-8.[17] The undulator beam was monochromatized by a Si (111) double-crystal monochromator, and energy band width was reduced further by a 4-bounce channel-cut Si (400) monochromator. Horizontally scattered x-rays were analyzed in energy by a spherically bent Si (551) analyzer for the Ni K edge and by a Ge (733) analyzer

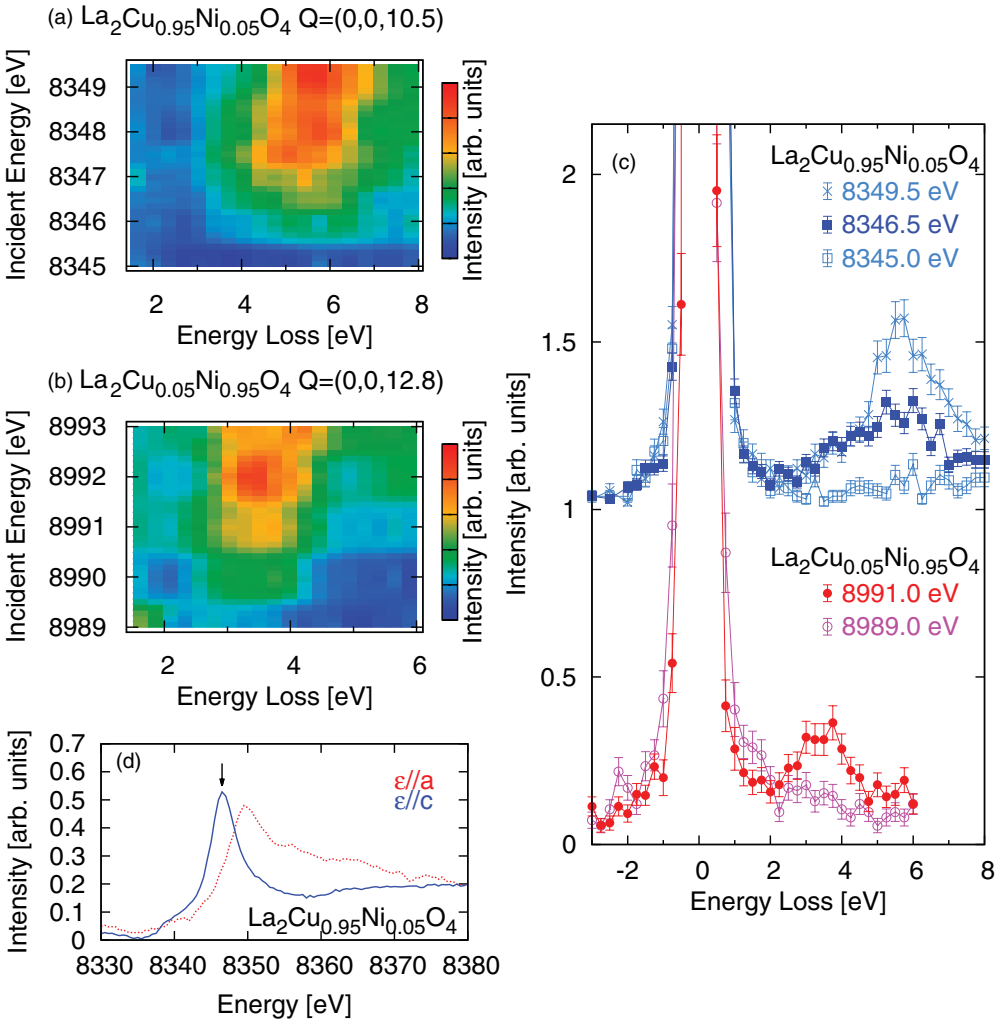

FIG. 1. (Color online) Incident photon energy dependence of RIXS spectra of (a) $La_2Cu_{0.95}Ni_{0.05}O_4$ near the Ni K edge and (b) $La_2Cu_{0.05}Ni_{0.95}O_4$ near the Cu K edge. The spectra at representative incident energies are plotted in (c). (d) Polarization-dependent Ni-K x-ray absorption spectra of $La_2Cu_{0.95}Ni_{0.05}O_4$. The arrow indicates the incident photon energy used for the measurement of momentum dependence.

for the Cu K edge. Total energy resolution estimated from the full width at half maximum is 350–450 meV.

Single crystals of $La_2Cu_{0.95}Ni_{0.05}O_4$ and $La_2Cu_{0.05}Ni_{0.95}O_4$ were grown by the traveling-solvent floating-zone method. The surface normal to the c axis was polished and irradiated by x-rays. The crystals were so mounted that the horizontal scattering plane is parallel to the ac plane. Polarization of the incident photon ($\boldsymbol{\epsilon}_i$) contains both in-plane ($\boldsymbol{\epsilon}_i \parallel \hat{\boldsymbol{a}}$) and out-of-plane ($\boldsymbol{\epsilon}_i \parallel \hat{\boldsymbol{c}}$) components in this experimental condition. Except for the momentum scan in Fig. 2, absolute momentum transfer ($\boldsymbol{Q}$) was parallel to the c^* axis. Throughout this paper, we use the tetragonal notation for the Miller indices, where the a/b axes are parallel to the Cu-O-Cu or Ni-O-Ni bond direction. In most cases the scattering angle (2θ) is close to 90°, where the elastic scattering is reduced due to the polarization factor of the Thomson scattering. All data are taken at room temperature.

III. EXPERIMENTAL RESULTS

Figures 1(a) and 1(b) show the incident energy dependence of the RIXS spectra, respectively, measured for $La_2Cu_{0.95}Ni_{0.05}O_4$ and $La_2Cu_{0.05}Ni_{0.95}O_4$. The momentum transfer is fixed at $\boldsymbol{Q} = (0,0,10.5)$ and $(0,0,12.8)$, respectively. As the incident energy passes through the absorption edge of the substituted element (∼8345 eV for Ni and ∼8989 eV for Cu), resonantly enhanced excitations clearly emerge. We also plot the spectra at representative incident energies in Fig. 1(c). It is clear in $La_2Cu_{0.95}Ni_{0.05}O_4$ that the spectral weight shifts to higher energy loss with increasing the incident energy. This shows that more than one excitation occurs within the measured incident energy range, with different resonant conditions. Starting with the spectrum measured for the highest incident energy, $E_i = 8349.5$ eV, we observe a prominent inelastic feature at 5.7 eV. By subtracting a scaled replica of this feature from the spectrum measured at $E_i = 8346.5$ eV, we obtain some residual spectral weight centered around 4 eV. We assign it to a second, distinct inelastic excitation, which we find disappears at $E_i = 8345$ eV. In order to focus on this low-energy excitation, we selected $E_i = 8346.5$ eV for the momentum-dependent measurements. Polarization(ϵ)-dependent x-ray absorption spectra (XAS) measured on $La_2Cu_{0.95}Ni_{0.05}O_4$ across the Ni K edge in the

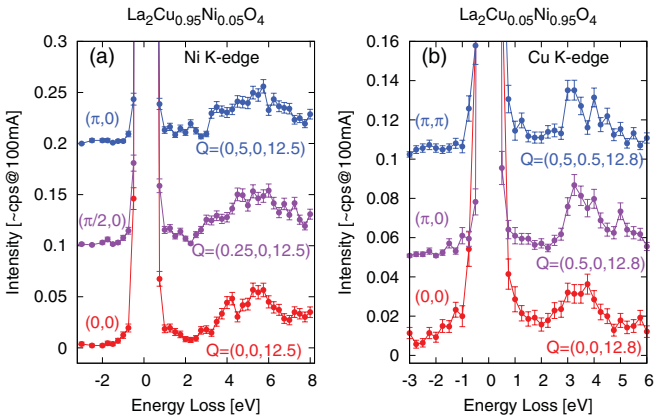

FIG. 2. (Color online) Momentum dependence of RIXS spectra of (a) $La_2Cu_{0.05}Ni_{0.95}O_4$ and (b) $La_2Cu_{0.95}Ni_{0.05}O_4$.

total fluorescence yield mode are shown in Fig. 1(d).[18] The spectra are not corrected for self-absorption since the fluorescence is predominantly absorbed by the La atoms. Both spectra are found to be similar to the ones of La_2NiO_4 .[19] The selected energy of 8346.5 eV is close to the maximum of the white line of the $\epsilon \parallel c$ spectrum, which is associated with the well-screened state of the $1s$–$4p_\pi$ transition. Turning now to the E_i dependence of $La_2Cu_{0.05}Ni_{0.95}O_4$ in Fig. 1(b), it is seen to be rather simple within the measured E_i region, as a single peak centered at 3.5 eV is observed. We chose $E_i = 8991$ eV for the momentum dependence. The energy coincides with the well-screened state of the $1s$–$4p_\pi$ transition in La_2CuO_4 and was used in the momentum-dependent measurements in Ref. 20.

The momentum dependence of the RIXS spectra is presented in Figs. 2(a) and 2(b). Absolute momentum transfers are $\boldsymbol{Q} = (H,0,12.5)$ for $La_2Cu_{0.95}Ni_{0.05}O_4$ and $\boldsymbol{Q} = (H,K,12.8)$ for $La_2Cu_{0.05}Ni_{0.95}O_4$, respectively. The momenta specified in left part of the figures are reduced to the first Brillouin zone. The spectra show little momentum dependence, which confirms that the observed excitations occur locally, or in the direct vicinity of the substituted site. In view of the limited statistics, we do not discuss the diplike features at 4.4 eV in the (0,0) spectra of $La_2Cu_{0.95}Ni_{0.05}O_4$ and at 3.75 eV in the (π,π) spectra of $La_2Cu_{0.05}Ni_{0.95}O_4$.

The RIXS spectra of $La_2Cu_{1-y}Ni_yO_4$ are compared for $y = 0$, 0.05, 0.95, and 1 in Fig. 3(a). The spectra of La_2CuO_4 and La_2NiO_4 are taken from Refs. 20 and 21, respectively. The momentum transfer is at the Brillouin zone center of the Cu(Ni)O_2 plane, and the incident energy is tuned to the well-screened state of the $1s$–$4p_\pi$ transition for all four spectra. Additionally, we also plotted the spectra at $(\pi,0)$ and (π,π) for La_2CuO_4, in order to show the large momentum dependence in this compound, contrasting with the momentum independence in the three other compounds. The upper two spectra of $y = 0$ and 0.95 are measured at the Cu K edge. In this case the core hole is created at the $1s$ orbital of the Cu site, and the observed excitation centered at 3 eV is ascribed to the CT excitation from O $2p$ to Cu $3d$. The CT excitations of $y = 0$ and 0.95 at the Cu K edge are schematically drawn in Figs. 3(b) and 3(c), respectively. On the other hand, the lower two spectra in Fig. 3(a) of $y = 0.05$ and 1 are measured at the Ni K edge, and therefore the CT excitation from O $2p$ to Ni $3d$ is observed, as shown in Figs. 3(d) and 3(e).

In Fig. 3(a) we notice that the center of mass of the spectral weight is somewhat similar between the upper two spectra and between the lower two spectra, respectively. It means that the CT excitation is locally unchanged at the substituted site. A more precise comparison of the spectra reveals that the onset edge of the CT excitation of La_2CuO_4 ($y = 0$) is lower in energy than that of $La_2Cu_{0.05}Ni_{0.95}O_4$ ($y = 0.95$). Similarly,

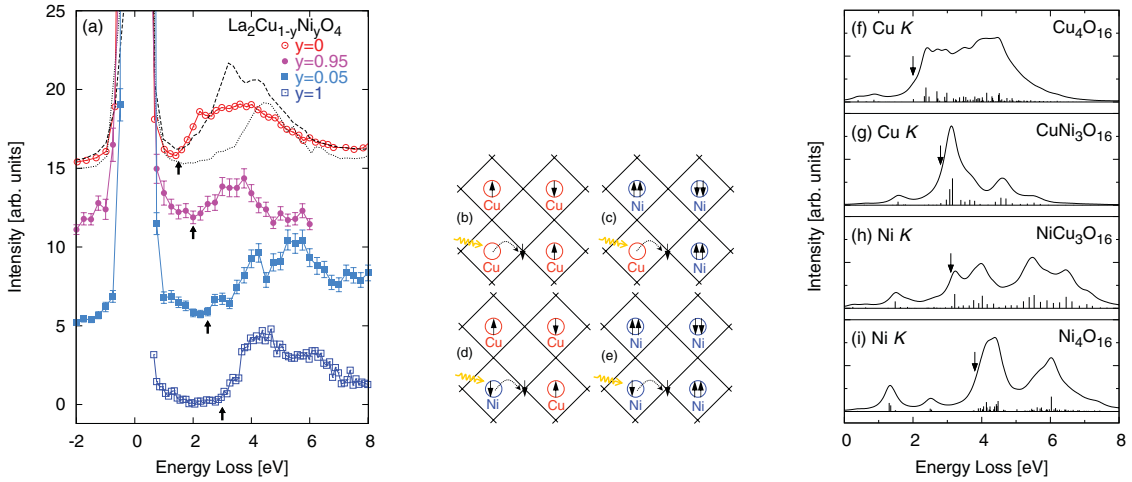

FIG. 3. (Color online) (a) RIXS spectra of $La_2Cu_{1-y}Ni_yO_4$ measured at the Brillouin zone center. The spectra of $y = 0$ and 1 are taken from the literature.[20,21] The upper and lower two spectra were measured at the Cu and Ni K edge, respectively. The dashed and dotted lines in $y = 0$ are the spectra at the momentum of $(\pi,0)$ and (π,π), respectively. The onset edges of the CT excitations are indicated by the arrows. Schematics of the charge transfer excitation in $La_2Cu_{1-y}Ni_yO_4$ with (b) $y = 0$, (c) 0.95, (d) 0.05, and (e) 1. Solid squares, open circles, and arrows denote CuO_4 (NiO_4) plaquettes, Cu (Ni) atoms, and holes, respectively. A core hole is created at the Cu or Ni atom by an incident photon (denoted by a wavy arrow) and a hole transfers to neighboring oxygen. The RIXS spectra calculated on $Cu_{4-y}Ni_yO_{16}$ clusters with $y = 0$ (f), 3 (g), 1 (h), and 4 (i). The spectra in (f, g) are at the Cu K edge and those in (h, i) are at the Ni K edge. Arrows indicate the leading edges of CT excitations.

the onset edge of $La_2Cu_{0.95}Ni_{0.05}O_4$ ($y = 0.05$) is lower than that of La_2NiO_4 ($y = 1$). The edges are indicated by the arrows in Fig. 3(a).

IV. THEORETICAL CALCULATION AND DISCUSSION

In order to analyze these results, we carried out calculations of the RIXS spectra by using the numerically exact diagonalization technique on $Cu_{4-y}Ni_yO_{16}$ clusters of the d-p model illustrated in Figs. 3(b)–(e). The models consist of $3d_{x^2-y^2}$ and $3d_{3z^2-r^2}$ orbitals for Cu and Ni sites and $2p_\sigma$ orbitals for O sites, which are located at the corners of the plaquettes, as well as $2p_z$ of both of the apex O's located along the $\pm z$ directions above and below the Cu and Ni sites, where the z direction is normal to the plaquette. The periodic boundary conditions are adopted in the clusters. Parameters included in the models are the hopping integrals between the $3d_{x^2-y^2}$ and the neighboring $2p_\sigma$ orbitals (T_{pd}), between $3d_{3z^2-r^2}$ and $2p_\sigma$ (T'_{pd}), and between $3d_{3z^2-r^2}$ and $2p_z$ (T''_{pd}); the intra- (U), interorbital (U') Coulomb repulsive and the exchange (K) interactions at the Ni/Cu $3d$ site; and finally the CT energy between Cu and O (Δ) and that between Ni and O ($\Delta_{\rm Ni}$)[12]. Here we set that $T_{pd} = \sqrt{3}T'_{pd} = \frac{\sqrt{3}}{2}T''_{pd}$ and $U = U' + 2K$. The RIXS spectrum is expressed as a second-order process of the dipole transition between Cu/Ni $1s$ and $4p$ orbitals, where the Coulomb interaction (U_c) between the core hole and $3d$ holes is explicitly included in the process. The parameters are set to be $T_{pd} = 1$, $U = 8$, $K = 0.8$, $\Delta = 3$, $\Delta_{\rm Ni} = 4.4$, $U_c = 4$, and the inverse of the lifetime of the intermediate states $\Gamma = 1$ in unit of eV, which are the same values as in our previous study.[12]

Figures 3(f)–(i) show the RIXS spectra calculated for $Cu_{4-y}Ni_yO_{16}$ clusters with $y = 0$ (f), 3 (g), 1 (h), and 4 (i). The RIXS spectra in panels (f) and (g) are at the Cu K edge, and those in panels (h) and (i) are at the Ni K edge. A good agreement is obtained between the calculated spectral weight distribution of the CT excitations and the experimentally observed one above 2 eV. For comparison with Fig. 3(a), Figs. 3(f)–(i) correspond to $y = 0$, 0.95, 0.05, and 1 of $La_2Cu_{1-y}Ni_yO_4$, respectively. The leading edge positions indicated by arrows in Figs. 3(f)–(i) are consistent with the ones in the experimental spectra in Fig. 3(a). The Ni K-edge RIXS spectrum calculated for 12.5% Ni doping, shown in Fig. 3 of Ref. 12, has its edge position at ~3 eV, which is very close to that of the spectrum calculated for 25% Ni doping in Fig. 3(h). This suggests that the edge position is not extremely sensitive to the doping rate, and that accordingly the spectra calculated for 25% Ni doping can be compared with the experimental spectrum for 5% Ni doping in Fig. 3(a). We note that the low-energy spectral structures at ~1 eV in Fig. 3(f), ~1.5 eV in panels (g) and (h), and ~1.5 and ~2.5 eV in panel (i) of Figs. 3 are associated with the so-called dd excitations.

The onset edge of the CT feature is understood as arising from an oxygen $2p$ hole transferred from a Cu/Ni $3d$ orbital at the core-hole-created site, forming the Zhang-Rice bound state with the $3d$ hole(s) of the neighboring metal site. Thus we consider the local density of states for d electrons (unoccupied states) at the core-hole-created site and for p holes (occupied states) at neighboring sites as illustrated in Fig. 4.

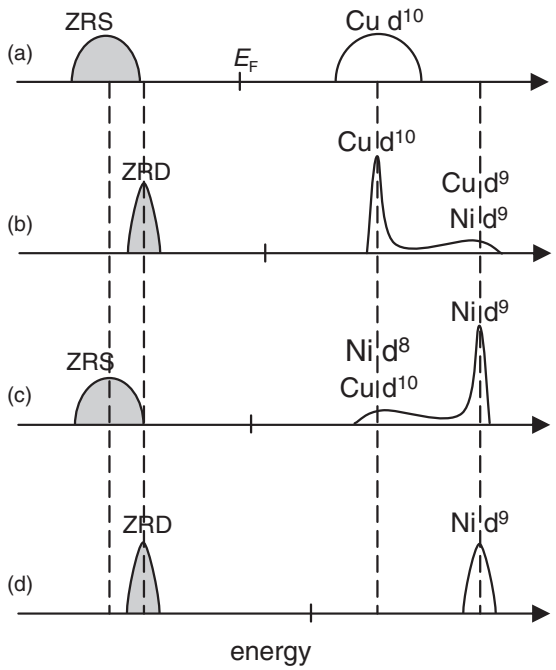

FIG. 4. Schematic local density of states (LDOS) for $La_2Cu_{1-y}Ni_yO_4$ with $y = 0$ (a), 0.95 (b), 0.05 (c), and 1 (d). Vertical ticks between the white and shaded structures indicate the Fermi level. White areas denote the LDOS above the Fermi level at the core-hole-created site, i.e. the Cu site in (a,b) and the Ni site in (c,d). Shaded areas denote the LDOS below the Fermi level at the neighboring oxygen sites. Broken lines represent the energy positions of the Zhang-Rice singlet (ZRS), the Zhang-Rice doublet (ZRD), the Cu $3d^{10}$ state, and the Ni $3d^9$ state, respectively, from left to right.

The unoccupied Cu $3d^{10}$ state is located at a lower energy than the Ni $3d^9$ states, while the difference of the occupied Zhang-Rice bound states is less prominent. This roughly explains the lower-energy position of the CT excitation of the upper two (Cu K edge) cases than that of lower two (Ni K edge). In addition, in the case of Fig. 4(a), the hopping of the Cu $3d^{10}$ site results in a gain of kinetic energy, which lowers the edge position of the unoccupied state compared with the substituted case [Fig. 4(b)], where there is no hopping. In the Ni K edge cases [Fig. 4(c) and 4(d)], the hopping of the Ni $3d^9$ site is less substantial because the effective hopping energy is smaller than that for Cu $3d^{10}$. Instead, in the case of Fig. 4(c), the energy of the unoccupied Ni $3d^9$ states is higher than that of the unoccupied Cu $3d^{10}$ state. That is, in the single-particle excitation spectrum, the Cu $3d^{10}$ state hybridized with Ni $3d^8$ appears at a lower excitation energy than that of the Ni $3d^9$ hybridized with neighboring Cu $3d^9$. In fact, the single-particle excitation spectra calculated for the same cluster models support the above discussion. Thus, the fact that the edge of the CT excitation in Fig. 3(h) is lower in energy than that in Fig. 3(i) comes from the hybridization effect in the unoccupied state at the substituted Ni site.

Our analysis shows that the effect of surrounding atoms on the unoccupied states of a substitute can be precisely examined using RIXS. This suggests that RIXS could be used as a probe to investigate whether substituted atoms are clustered

or uniformly distributed: If Ni atoms form clusters in the Ni-substituted cuprate, the Ni K-edge RIXS spectrum should show an edge position similar to that in the pure-nickelate case. The difference in edge position between $y = 0.05$ and 1 in Fig. 3(a) indicates that the substituted Ni atoms are not clustered in the $y = 0.05$ samples. We note that the miscibility of the substituted atoms, namely, whether the Ni atoms are uniformly distributed or clustered, also may be examined with a precise EXAFS experiment from a structural viewpoint.[22]

V. SUMMARY

We have carried out a resonant inelastic x-ray scattering study of Ni-substituted La_2CuO_4 and Cu-substituted La_2NiO_4. The capability of RIXS to investigate the local excitations around the substituted element was demonstrated; that is, electronic excitations in $La_2Cu_{0.95}Ni_{0.05}O_4$ and $La_2Cu_{0.05}Ni_{0.95}O_4$ were successfully observed at the K edge of the substituted element. When the incident photon energy is tuned to the well-screened core hole state, CT excitations from O $2p$ to substituted Cu or Ni $3d$ states appear in the spectra. Their momentum dependence is small. The edge position of the CT excitations is found to be different between the bulk state and the substitute state even if the same element is targeted by RIXS. The difference in energy is quantitatively reproduced by a theoretical calculation based on a d-p model. We conclude that RIXS on the substituted atoms can be useful for exploring their electronic states affected by their surroundings.

ACKNOWLEDGMENTS

We would like to thank D. Matsumura for invaluable discussions. This work was performed under the interuniversity cooperative research program of the Institute of Materials Research, Tohoku University, and financially supported by Grant-in-Aids for Scientific Research from the MEXT and JPSJ. Computations were partly carried out in YITP, Kyoto University, and ISSP, University of Tokyo.

[1] J. P. Attfield, A. L. Kharlanov, and J. A. McAllister, Nature (London) **394**, 157 (1998).
[2] K. Fujita, T. Noda, K. M. Kojima, H. Eisaki, and S. Uchida, Phys. Rev. Lett. **95**, 097006 (2005).
[3] H. Alloul, J. Bobroff, M. Gabay, and P. J. Hirschfeld, Rev. Mod. Phys. **81**, 45 (2009).
[4] W. Kang, H. J. Schulz, D. Jérome, S. S. P. Parkin, J. M. Bassat, and P. Odier, Phys. Rev. B **37**, 5132 (1988).
[5] G. Xiao, M. Z. Cieplak, J. Q. Xiao, and C. L. Chien, Phys. Rev. B **42**, 8752 (1990).
[6] H. Fujishita and M. Sato, Solid State Commun. **72**, 529 (1989).
[7] V. Bhat, C. N. R. Rao, and J. M. Honig, Physica C **191**, 271 (1992).
[8] T. Nakano, N. Momono, T. Nagata, M. Oda, and M. Ido, Phys. Rev. B **58**, 5831 (1998).
[9] H. Hiraka, S. Ohta, S. Wakimoto, M. Matsuda, and K. Yamada, J. Phys. Soc. Jpn. **76**, 074703 (2007).
[10] M. Matsuda, M. Fujita, and K. Yamada, Phys. Rev. B **73**, 140503 (2006).
[11] H. Hiraka, D. Matsumura, Y. Nishihata, J. Mizuki, and K. Yamada, Phys. Rev. Lett. **102**, 037002 (2009).
[12] K. Tsutsui, A. Toyama, T. Tohyama, and S. Maekawa, Phys. Rev. B **80**, 224519 (2009).
[13] S. H. Pan, E. W. Hudson, K. M. Lang, H. Eisaki, S. Uchida, and J. C. Davis, Nature (London) **403**, 746 (2000).
[14] E. W. Hudson, K. M. Lang, V. Madhavan, S. H. Pan, H. Eisaki, S. Uchida, and J. C. Davis, Nature (London) **411**, 920 (2001).
[15] A. Kotani and S. Shin, Rev. Mod. Phys. **73**, 203 (2001).
[16] L. J. P. Ament, M. van Veenendaal, T. P. Devereaux, J. P. Hill, and J. van den Brink, Rev. Mod. Phys. **83**, 705 (2011).
[17] Y. Q. Cai, P. Chow, C. C. Chen, H. Ishii, K. L. Tsang, C. C. Kao, K. S. Liang, and C. T. Chen, AIP Conf. Proc. **705**, 340 (2004).
[18] It is difficult to measure the absorption spectra of $La_2Cu_{0.05}Ni_{0.95}O_4$ at the Cu K edge in the total fluorescence yield mode because of the strong fluorescence background from Ni, but the line shape can be reasonably expected to be similar to that of La_2CuO_4.
[19] A. Sahiner, M. Croft, S. Guha, I. Perez, Z. Zhang, M. Greenblatt, P. A. Metcalf, H. Jahns, and G. Liang, Phys. Rev. B **51**, 5879 (1995).
[20] Y. J. Kim, J. P. Hill, C. A. Burns, S. Wakimoto, R. J. Birgeneau, D. Casa, T. Gog, and C. T. Venkataraman, Phys. Rev. Lett. **89**, 177003 (2002).
[21] E. Collart, A. Shukla, J.-P. Rueff, P. Leininger, H. Ishii, I. Jarrige, Y. Q. Cai, S.-W. Cheong, and G. Dhalenne, Phys. Rev. Lett. **96**, 157004 (2006).
[22] Practically, it is rather difficult in the present case to distinguish whether the substituted atoms are clustered or uniformly distributed with EXAFS. First, the distinction between Cu and Ni in EXAFS is hard because their atomic numbers are similar. Second, the distance between the nearest neighbor Cu (Ni) atoms is close to that between La and Cu (Ni), which makes the analysis of EXAFS oscillation difficult.